

CIRCUMFERENCE CORRECTION CHICANES FOR DAMPING RINGS*

P. Emma and T.O. Raubenheimer

Stanford Linear Accelerator Center, Stanford University, Stanford, CA 94309, USA

1 INTRODUCTION

Several low-emittance damping rings are presently being designed to meet the requirements of future linear colliders. These rings tend to have relatively large circumferences ~ 300 m so that they can damp many trains of bunches at the same time. With the large circumference, the ring path length may become quite sensitive to thermal and ground motion effects. In addition, most of the rings include damping wigglers whose path length varies with their strength.

In e^-/e^+ storage rings, the beam revolution time is determined by the rf frequency. Thus, to restore the proper revolution time, a change in the nominal path length will cause a change in both the beam energy and the closed orbit. The change in energy is given by:

$$\frac{dE}{E_0} = -\frac{1}{\alpha_p} \frac{\Delta C}{C_0}, \quad (1)$$

where α_p is the momentum compaction and C_0 is the nominal ring circumference. The change in the closed orbit is simply given by the energy change and the dispersion function. This change in orbit and energy can decrease the dynamic acceptance of the ring and make it difficult to preserve the ultra-small damped emittances. Because damping rings need strong focusing to attain the small beam emittances and thus tend to have very small values of momentum compaction, they can be very sensitive to changes in their circumference. For example, to limit the energy fluctuations in the NLC damping rings to 10% of the beam equilibrium energy spread, the path length must be controlled to about $20 \mu\text{m}$.

Circumference variations have been seen at most storage rings including LEP, the APS at Argonne, the SLAC damping rings, and the ATF damping ring test facility [1] at KEK. At the APS, typical path length variations are ~ 0.2 mm [2] and are correlated with seasonal, tidal, and diurnal fluctuations. The SLAC damping rings change by millimeters during approach to thermal equilibrium when the rings are started, but little variation is seen after equilibrium is reached. At the ATF, variations of up to ± 3 mm over months have been observed [3]. The precise mechanisms responsible for these changes are not, at present, well understood.

Another path length variation arises when the strength of the damping wigglers is changed. Assuming a sinusoidal wiggler field, the circumference change is

$$\Delta C \approx \frac{1}{4} \frac{L_w}{\rho_w^2 \kappa_w^2}, \quad (2)$$

where L_w is the wiggler length, ρ_w is the peak wiggler bend radius, and κ_w is its wavenumber ($\equiv 2\pi/\lambda$). At the ATF (and similarly for the NLC ring), the wigglers increase the circumference by ~ 2 mm at full strength.

Although some of the variation in path length can probably be reduced by design, the inclusion of a circumference correction method in the design of future damping rings seems prudent. There are a few possible approaches: 1) physical displacement of the arc magnetic elements; 2) control of the orbit using steering correctors or, equivalently, variation of the arc bending magnets and quadrupoles (the later is necessary to keep tunes constant); and 3) additional elements dedicated to path length control. In this note, we describe the correction available by adding a simple 4-dipole chicane to a straight-section in a damping ring. A chicane has the advantage of being varied without significantly affecting ring optics or trajectory outside of the chicane. Thus, the path length can be varied during operation and the chicane can be used in a feedback system to stabilize the circumference. In the following, we describe the effects of the chicane on critical ring parameters, including the equilibrium emittance and momentum compaction.

2 CHICANE IMPACT ON DAMPING RING PERFORMANCE

A standard 4-dipole chicane is shown in Figure 1 where the symbol definitions are indicated.

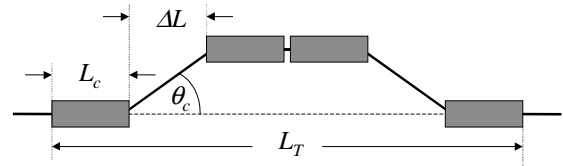


Figure 1: Four dipole chicane with symbol definitions indicated.

2.1 Path Length

For an ‘on-energy’ particle through this chicane, the change in path length (*i.e.* circumference), with respect to the path length with no chicane, and for $\theta_c \ll 1$, is

$$\Delta s \approx \theta_c^2 \left(\frac{2}{3} L_c + \Delta L \right). \quad (3)$$

Note that Δs is always positive so that providing a bipolar circumference correction requires a chicane with a

* Work supported by Department of Energy, contract DE-AC03-76SF00515.

nominal bias at nominal circumference (*i.e.* $\theta_c = \theta_{c_0} \neq 0$). The path length is then increased (decreased) by an increase (decrease) of the dipole bend angles.

$$\Delta s_b \approx \left(\theta_c^2 - \theta_{c_0}^2 \right) \left(\frac{2}{3} L_c + \Delta L \right) \quad (4)$$

The subscript b is added to identify a bipolar correction from the unipolar one in Eq. (3), ($\Delta s_b = \Delta s - \Delta s_{\max}/2$).

2.2 Emittance

The addition of the chicane dipoles will, of course, have some impact on the damped horizontal emittance. The normalized equilibrium emittance for a damping ring, with chicane included, can be written as [4]

$$\gamma \mathcal{E} = \frac{C_q \gamma^3 I_5}{I_2 - I_4} = \frac{C_q \gamma^3}{J_x I_2} \cdot \frac{I_5 + \Delta I_5}{1 + \Delta I_2 / J_x I_2 - \Delta I_4 / J_x I_2}, \quad (5)$$

where I_j ($j = 2, 4, 5$) are the usual j^{th} synchrotron integrals, ΔI_j are their chicane induced changes, γ is the beam energy factor, J_x is the nominal horizontal partition, and $C_q \approx 3.8 \times 10^{-13}$ m. For an isomagnetic, uncoupled ring with the chicane of Figure 1, the first correction term ($\Delta I_2 / J_x I_2$) at the right-side of Eq. (5) can be expressed as

$$\frac{\Delta I_2}{J_x I_2} = \frac{4}{N_B} \cdot \frac{\tau_x}{\tau_y} \cdot \frac{L_B}{L_c} \cdot \frac{\theta_c^2}{\theta_B^2} \cdot \frac{1}{1 + F_w} \ll 1, \quad (6)$$

where F_w (≥ 0) is the ratio of the energy loss per turn in the wiggler to that in the arcs (typically ~ 1), $\tau_x \tau_y$ ($= 1/J_x$) is the ratio of horizontal to vertical damping times (typically ~ 1), L_B and θ_B are length and bend angle of an arc dipole, and N_B is the number of arc dipoles in the ring (typically $\gg 1$). As will be demonstrated, Eq. (6) is ~ 0.01 for a chicane with $\Delta s_{\max} = 5$ mm placed in the 1.54 GeV ATF damping ring with wigglers switched on (see Table 1). Thus, this ΔI_2 term in the denominator of Eq. (5) can typically be ignored. Similarly, the ΔI_4 term in the denominator is related to Eq. (6) by

$$\frac{\Delta I_4}{J_x I_2} \approx \left(\frac{L_c + \Delta L}{2L_c} \right) \cdot \frac{\Delta I_2}{J_x I_2} \cdot \theta_c^2 \ll 1, \quad (7)$$

which is smaller yet. For the ATF case above, Eq. (7) is $\sim 6 \times 10^{-5}$, so this term is completely insignificant. These synchrotron integrals are not significantly changed by a reasonable chicane and, therefore, damping times, losses per turn, and partition numbers are also nearly unaffected. With these results, Eq. (5) becomes

$$\gamma \mathcal{E} \approx \frac{C_q \gamma^3}{J_x I_2} (I_5 + \Delta I_5), \quad (8)$$

where J_x and I_2 are the nominal horizontal partition and 2nd synchrotron integral of the pre-chicane ring, including wigglers, and the ΔI_5 -term is the change in the nominal equilibrium emittance due to the chicane.

The change in the 5th synchrotron integral is

$$\Delta I_5 = \frac{L_c}{|\rho_c|^3} \sum_i \left\langle \eta_i^2 \gamma_i + 2\alpha_i \eta_i \eta_i' + \eta_i'^2 \beta_i \right\rangle, \quad (9)$$

where ρ_c ($\equiv L_c/\theta_c$) is the bend radius of the chicane dipoles, η_i and η_i' are the spatial and angular dispersion functions through each dipole, γ_i , β_i , and α_i are the Twiss parameters through each dipole, and the brackets denote the mean value over the length of each dipole. It can be shown that for a small initial α -function (at 1st dipole entrance), $|\alpha_1(0)| < 1$, and a initial β -function which satisfies $\beta_1(0) > L_c + \Delta L$, Eq. (9) reduces approximately to

$$\Delta I_5 \approx \frac{4L_c}{|\rho_c|^3} \bar{\beta} \langle \eta'^2 \rangle = \frac{4|\theta_c|^3}{L_c^2} \bar{\beta} \langle \eta'^2 \rangle, \quad (10)$$

where $\bar{\beta}$ -bar is the mean beta function over all dipoles. (For small $|\alpha|$, the β -function is nearly constant.) In a symmetric chicane, the angular dispersion, $\eta(s) = s/\rho_c$, is equal in all dipoles and its mean-squared value over L_c is $\langle \eta'^2 \rangle = \theta_c^2/3$. Eq. (3) is now used to substitute for θ_c , and relations for the nominal 2nd synchrotron integral and horizontal partition are introduced.

$$I_2 = \frac{3C_0}{r_e c \gamma^3 \tau_y}, \quad J_x = \frac{\tau_y}{\tau_x} \quad (11)$$

Here, r_e is the classical electron radius and c is the speed of light. The length of the chicane is defined as $L_T \equiv 4L_c + 2\Delta L$. (This definition does not include a potential small drift between center bends which has no effect on these results.) With these relations added, the change in the nominal emittance from Eq. (8) becomes

$$\Delta \gamma \mathcal{E} \approx \frac{4}{9} C_q r_e c \cdot \frac{\tau_x \bar{\beta} \gamma^6}{C_0} \cdot \frac{\Delta s^{5/2}}{L_c^2 (L_T/2 - 4L_c/3)^{5/2}}. \quad (12)$$

The 6th power scaling in γ holds only for a constant τ_x . The emittance increase is minimum at $L_c = \Delta L = L_T/6$ and

$$\Delta \gamma \mathcal{E} \approx 393 \cdot C_q r_e c \cdot \frac{\tau_x \bar{\beta} \gamma^6}{C} \cdot \frac{\Delta s^{5/2}}{L_T^{9/2}}, \quad (13)$$

where the chicane must satisfy

$$|\theta_c| \approx 3 \sqrt{\frac{2\Delta s}{5L_T}}, \quad L_c = L_T/6 = \Delta L. \quad (14)$$

Eq. (13) is the equilibrium emittance increase produced by adding, to a damping ring, a chicane with additional path length Δs . Numerical results are described below.

2.3 Momentum Compaction

The effect on momentum compaction of the ring is

$$\alpha_p = \alpha_{p_0} - 2 \frac{\Delta s}{C_0}, \quad (15)$$

with α_{p_0} the nominal momentum compaction. This is typically a very small change in α_p and also indicates that

the chicane's effect on the extracted bunch length ($\propto \alpha_p^{1/2}$) is insignificant.

2.4 Energy Spread

Finally, the relative change in the 3rd synchrotron integral is given by

$$\frac{\Delta I_3}{I_3} = \frac{4}{N_B} \cdot \frac{L_B^2}{L_c^2} \cdot \left| \frac{\theta_c}{\theta_B} \right|^3 \ll 1. \quad (16)$$

For the ATF chicane described above, Eq. (16) is 0.074. In consideration of the small impact on I_2 and insignificant change in I_4 shown in Eqs. (6-7), the chicane's impact on the ring's energy spread can be approximated by

$$\sigma_\delta \approx \sigma_{\delta_0} \sqrt{1 + \frac{4}{N_B} \cdot \frac{L_B^2}{L_c^2} \cdot \left| \frac{\theta_c}{\theta_B} \right|^3 \left[1 - \frac{2}{J_\epsilon (1 + F_w)} \cdot \left| \frac{\theta_B}{\theta_c} \right| \frac{L_c}{L_B} \right]}, \quad (17)$$

where $J_\epsilon = 3 - \tau_y/\tau_x$. Eq. (17) shows that the energy spread can increase or decrease, depending on parameters.

3 ATF DAMPING RING

Parameters of the ATF and NLC damping rings, with wigglers switched on, are listed in Table 1.

Table 1: ATF and NLC damping ring parameters with wigglers on and no chicane.

Parameter	sym.	unit	ATF	NLC
Beam energy	E	GeV	1.54	1.98
Arc-dipole magnet length	L_B	m	1.0	1.07
Arc-dipole bend angle	θ_B	deg	10.0	10.6
Total no. of arc-dipoles	N_B	—	36	34
Equilibrium X emit. (rms)	$\gamma\epsilon_0$	μm	4.3	2.4
Horizontal damping time	τ_x	msec	6.8	5.2
Vertical damping time	τ_y	msec	9.1	5.2
Mean beta at chicane	$\langle\beta\rangle$	m	~ 10	~ 6
Ring circumference	C_0	m	139	282
Ratio wiggler to arc E -loss	F_w	—	1.6	2
Rel. energy spread (rms)	σ_δ	0.1 %	0.72	0.91
Momentum compaction	α_{p_0}	—	1.9	0.58

In order to fit such a chicane into the existing ATF lattice requires a free beamline section of length $\geq L_T$. In the ATF, a 2.1-meter space can be made available by removing one of eight wiggler sections. In this case, ($L_T = 2$ m) the range of $\Delta s_b = \pm 1$ mm correction is possible with a maximum emittance increase (at $\Delta s_b = +1$ mm) of $\sim 8\%$ at 1.54 GeV. This is a fairly small circumference correction in light of the ± 3 mm variations observed. It may, however, be possible to add two 2-meter chicanes which will double both the Δs_b range and the emittance increase. This should be compared with doubling the Δs_b range using a single, stronger chicane. The latter method multiplies the emittance increase by $2^{5/2} \approx 5.7$. The double chicane, however, requires the elimination of 25% of the ATF wiggler which will increase the vertical

damping time by $\sim 20\%$. A simple solution which provides a ± 3 -mm correction does not appear to be viable.

4 NLC MAIN DAMPING RING

Parameters of the 3-bunch train NLC main damping ring used here are listed in Table 1. These parameters represent a recent proposal which includes 40-meters of wiggler in order to increase the net momentum compaction to $> 5 \times 10^{-4}$.

In order to provide a ± 1 mm circumference correction range for the NLC ring requires a single chicane of $L_T = 2.6$ m, $\theta_{c\text{max}} = 3^\circ$, with $\Delta\epsilon/\epsilon_0 \approx 6\%$ at $\Delta s_b = +1$ mm. Two such chicanes can provide a ± 2 mm range with a 12% maximum growth, or a ± 1.5 mm range at a 6% maximum growth. Figure 2 shows the relative emittance increase for the NLC main damping ring, using Eq. (13), for chicane lengths of 1, 2, 3, 4, and 5 meters versus unipolar circumference correction, Δs .

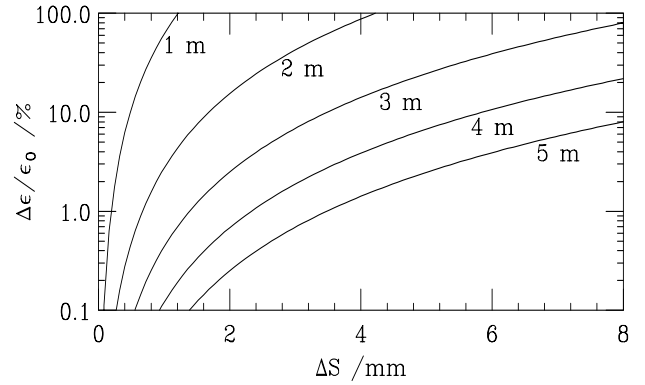


Figure 2: Relative equilibrium emittance increase vs. circumference change for NLC main damping ring with chicane lengths, L_T , of 1, 2, 3, 4, and 5 meters at 1.98 GeV, $\langle\beta\rangle = 6$ m, $\gamma\epsilon_0 = 2.4 \mu\text{m}$, $\tau_x = 5.2$ msec.

The effect of a double chicane for the NLC can be estimated if both horizontal and vertical scales of Figure 2 are multiplied by 2. In this case Δs is the total path length change and $\Delta\epsilon/\epsilon_0$ is the total emittance increase. Providing more than ± 2 mm correction range for the NLC using only chicanes may be problematic. Larger corrections, although not clearly necessary, can be generated by either displacing ring components or by changing arc magnet excitation levels.

5 REFERENCES

- [1] J. Urakawa, "KEK/ATF Damping Ring", PAC97, Vancouver, B.C., Canada, (1997).
- [2] M. Ross, M. Borland, private communication (1998).
- [3] Report on 4th International Collaboration Meeting, July 17, 1998, J. Urakawa editor, internal note.
- [4] R.H. Helm, et. al., "Evaluation of Synchrotron Radiation Integrals", SLAC-PUB-1193 (A), March 1973.